Monatshefte für Chemie (2002)
DOI 10.1007/s00706-002-0510-y

Monatshefte für Chemie
Chemical Monthly
Printed in Austria

Invited Review

Cross-Polarisation Applied to the Study of Liquid Crsytalline Ordering

Krishna V. Ramanathan[1,*] and **Neeraj Sinha**[2]

[1] Sophisticated Instruments Facility, Indian Institute of Science, Bangalore-560012, India
[2] Department of Physics, Indian Institute of Science, Bangalore-560012, India

Received May 28, 2002; accepted June 19, 2002
Published online October 7, 2002

Summary. Cross polarisation is extensively used in solid state NMR for enhancing signals of nuclei with low gyromagnetic ratio. However, the use of the method for providing quantitative structural and dynamics information is limited. This arises due to the fact that the mechanism which is responsible for cross polarisation namely, the dipolar interaction, has a long range and is also anisotropic. In nematic liquid crystals these limitations are easily overcome since molecules orient in a magnetic field. The uniaxial ordering of the molecules essentially removes problems associated with the angular dependence of the interactions encountered in powdered solids. The molecular motion averages out intermolecular dipolar interaction, while retaining partially averaged intramolecular interaction. In this article the use of cross polarisation for obtaining heteronuclear dipolar couplings and hence the order parameters of liquid crystals is presented. Several modifications to the basic experiment were considered and their utility illustrated. A method for obtaining proton–proton dipolar couplings, by utilizing cross polarisation from the dipolar reservoir, is also presented.

Keywords. Cross-polarisation; Liquid crystals; Dipolar couplings; Ordering; Order parameter.

Introduction

Dipolar couplings have been one of the major sources of information for the study of liquid crystalline ordering [1–3]. While proton dipolar couplings have been used extensively in the case of small molecules with up to about ten spins oriented in liquid crystalline media, for larger molecules and for the liquid crystals themselves the method has been of very limited use. On the other hand, heteronuclear dipolar couplings pose a lesser problem in terms of line-width and resolution, and therefore offer an attractive means of studying liquid crystalline ordering. One of the first demonstrations of this approach has been made with the study of ^{2}H–^{13}C dipolar

* Corresponding author. E-mail: kvr@sif.iisc.ernet.in

couplings in *N*-(4-methoxy-benzylidene)-4-*n*-butylaniline (*MBBA*) deuterated at a specific site [4]. Similar studies have been performed on systems containing ^{19}F and using ^{19}F–^{13}C dipolar couplings [5, 6]. However, a more general and attractive approach would be to utilize ^{1}H–^{13}C dipolar couplings. The use of the 2D SLF procedure for this purpose was first demonstrated for the case of *MBBA* by *Hohener et al.* [4]. The ^{13}C chemical shifts and the corresponding ^{13}C–^{1}H dipolar splittings have been displayed along the F_2 and F_1 axes. However, in this method, the presence of the homonuclear dipolar couplings tend to make the lines broad along the F_1 axis. The problem of the elimination of the proton–proton dipolar couplings has been addressed by employing the variable angle sample spinning (VASS) technique [7]. Due to the off-magic angle spinning, the proton dipolar coupling is significantly reduced and further use of the multiple pulse decoupling during the t_1 period enables near elimination of proton dipolar couplings. The ^{13}C–^{1}H dipolar splittings observed along F_1 are to be suitably scaled to include the effect of VASS and the multiple pulse decoupling, to obtain the actual dipolar couplings. This method has been used for the study of a large number of liquid crystalline systems [8]. Modifications to this technique have also been suggested which enable short range [9] and long range [10, 11] dipolar couplings to be measured accurately.

Another approach that has been proposed and implemented is the use of a variant of the SLF 2D experiment that uses the transient oscillations observed during cross polarisation [12, 13] for estimating the dipolar couplings [14].

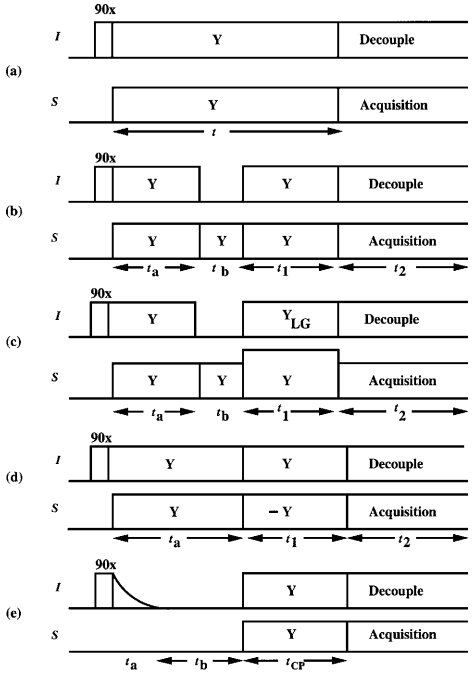

Fig. 1. Various cross-polarisation pulse schemes employed for obtaining dipolar couplings: (a) *Hartmann–Hahn* cross-polarisation, (b) cross-depolarisation, (c) cross-depolarisation with *Lee–Goldburg* decoupling, (d) polarisation inversion, (e) cross-polarisation from the dipolar bath

Modifications to the standard cross-polarisation pulse scheme such as the use of homonuclear decoupling during CP and the use of polarisation inversion have also been suggested [15, 16]. These are described in more detail in the following sections. A method of indirectly monitoring proton dipolar couplings using the carbon chemical shift dispersion has also been suggested which is also described. The various pulse schemes that have been utilized are shown in Fig. 1.

Dipolar Oscillations is Cross-Polarisation

Observation of dipolar oscillations during cross-polarisation (CP) has been made by *Muller et al.* in a single crystal of ferrocene [12]. In liquid crystals such as *MBBA* (Fig. 2), ^{13}C spectra containing sharp well-resolved lines can be obtained by the use of the CP sequence (Fig. 1a).

The intensity of the carbon lines show an oscillatory build-up when recorded as a function of the contact time t [14]. These oscillations are observed when the dipolar couplings of a carbon to its nearest neighbour protons are much stronger

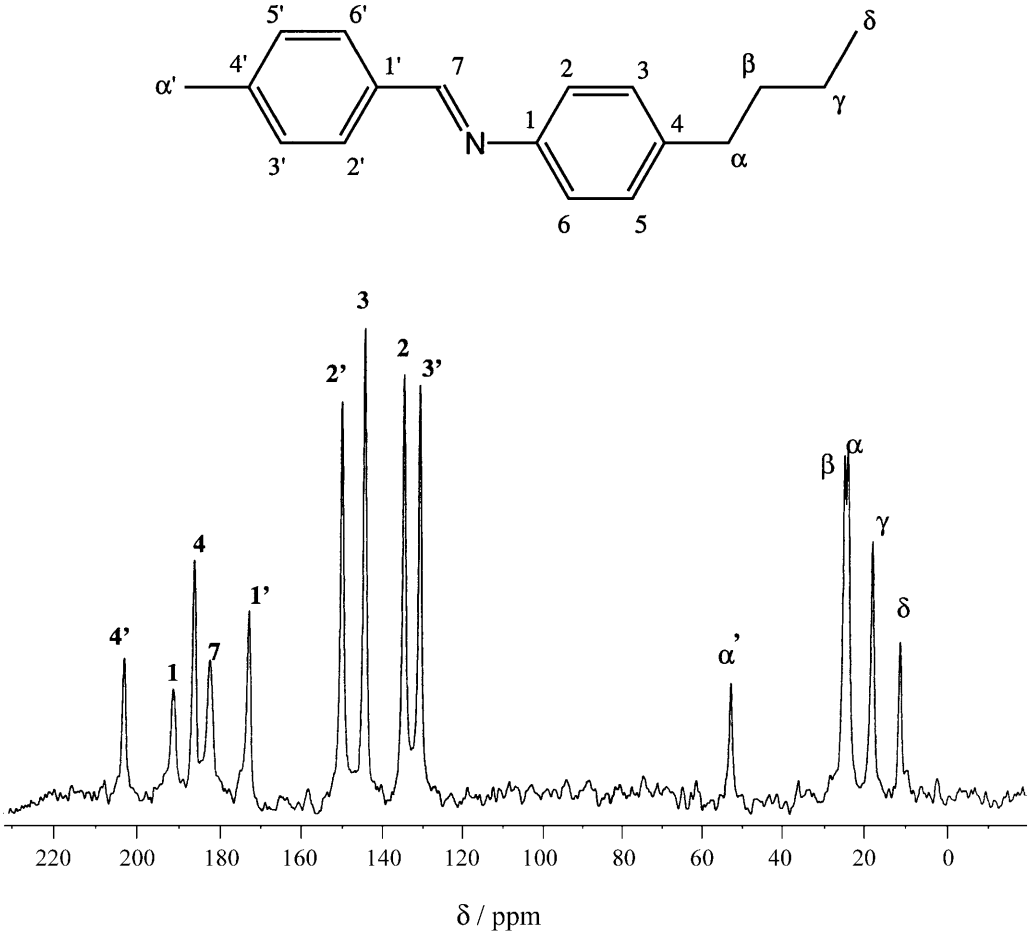

Fig. 2. Proton-decoupled ^{13}C spectrum of *MBBA* recorded on a Bruker DSX-300 NMR spectrometer at 75.47 MHz at room temperature

than the coupling of this spin system to the rest of the protons. The frequency f of the oscillations is given by

$$M_S = M_{S0}(1/2 - 1/2\cos(ft)). \tag{1}$$

The value of f is given in terms of D, the C–H dipolar coupling. It also depends on the number of equivalent protons coupled to a carbon. Thus for an IS spin system, such as a C–H group, $f = D$ and for the I_2S spin system such as the CH_2 group, $f = \sqrt{2}D$. For the methyl group (I_3S case), three values for f may be expected corresponding to D, $\sqrt{3}D$ and $2D$. Here the dipolar coupling D expressed in kHz is defined as

$$D = (-h\gamma_C\gamma_H/4\pi^2 r_{CH}^3)S_{CH} \tag{2}$$

where γ_H, γ_C are the gyromagnetic ratios of the protons and carbons respectively, r_{CH} is the internuclear vector and S_{CH} is the order parameter along the direction of this vector. The value of $(h\gamma_C\gamma_H/4\pi^2 r_{CH}^3)$ is 22.68 kHz for $r_{CH} = 1.1$ Å. Equation (1) is further modified [12] to take into account spin diffusion between the protons directly coupled to the carbon under consideration and the rest of the protons in the system as

$$M_S = M_{S0}[1 - 1/2\exp(-t/T_{II}) - 1/2\exp(-3t/T_{II})\cos(ft)] \tag{3}$$

where T_{II} represents the time constant for the spin diffusion process.

Figure 2 shows the proton decoupled ^{13}C spectrum of *MBBA* at room temperature. Figure 3 presents the variation of the intensities of the C_7, C_α, C_β, and C_γ carbons as a function of the contact time. The oscillation frequency f and hence dipolar coupling D can be obtained by fitting Eq. (3) to the experimental data.

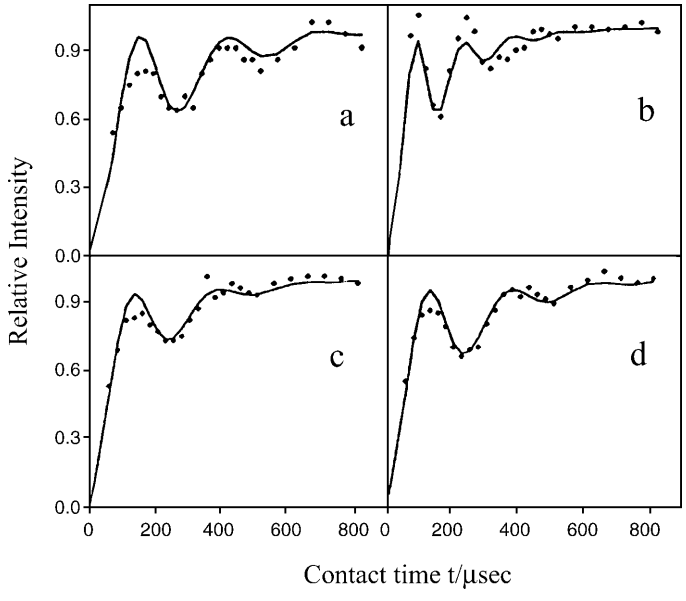

Fig. 3. Relative intensities of signals of (a) C_7, (b) C_α, (c) C_β, and (d) C_γ carbons of *MBBA* plotted against contact time. Points correspond to experimental values and the continuous line corresponds to the fit of the data to Eq. (3) with (a) $f = 3.73$ kHz, $T_{II} = 333$ μs, (b) $f = 6.84$ kHz, $T_{II} = 181$ μs, (c) $f = 3.90$ kHz, $T_{II} = 228$ μs, and (d) $f = 4.0$ kHz, $T_{II} = 273$ μs

Values of 3.73, 4.84, 2.76, and 2.84 kHz were obtained for D respectively for the C_7, C_α, C_β, and C_γ carbons of *MBBA*. The C_7 dipolar coupling enables the order parameter S of the aromatic core to be estimated with the assumption of uniaxial ordering from

$$D = -S(h\gamma_C\gamma_H/4\pi^2 r_{CH}^3)(3\cos^2\theta - 1)/2 \tag{4}$$

where θ is the angle between the director and the C–H bond. Using a value of 114° for the C–C–H bond angle and assuming a tilt of the director by 3.5° from the *para*-axis of the adjacent phenyl ring a value of $S = 0.52$ was obtained from these measurements, which agrees well with values reported by using other methods. The magnitude of the order parameter along the aliphatic chain averaged over several conformations can also be calculated from Eq. (2) using the obtained values of dipolar couplings. Values of 0.21, 0.12, and 0.13 obtained for the carbon sites α β, and γ are in agreement with the variation of order parameter generally observed in liquid crystalline systems.

A straightforward way of obtaining the oscillation frequencies is to use the 2D approach where the CP contact time (t) is incremented in regular steps between successive experiments. A two-dimensional data set is collected with proton decoupling during t_2. A two-dimensional *Fourier* transform then gives ^{13}C chemical shifts along the F_2 axis and the oscillation frequencies along F_1. A cross-depolarisation experiment (Fig. 1b), rather than a cross-polarisation experiment provides better results, the axial peaks which arise from the non-oscillatory terms of Eq. (3) is less intense in the former case (*vide infra*). The S spin magnetization during the t_1 period is given by

$$M_S = M_{S0}[1/2\exp(-t_1/T_{II}) + 1/2\exp(-3t_1/T_{II})\cos(ft_1)]. \tag{5}$$

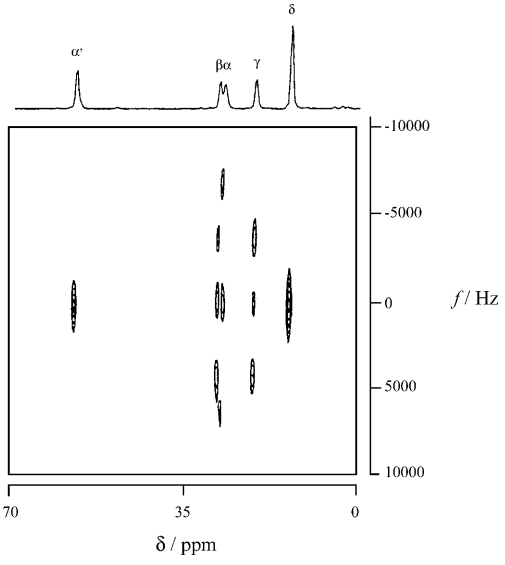

Fig. 4. Two-dimensional spectrum of the aliphatic carbons of *MBBA* obtained using the pulse sequence shown in Fig. 1b on a Bruker DSX-300 NMR spectrometer at 75.47 MHz at room temperature. The horizontal axis corresponds to ^{13}C chemical shifts and the vertical axis to the dipolar oscillation frequencies. The projection along the horizontal axis of the two-dimensional spectrum is also shown

The peaks along the F_1 axis provide the oscillation frequencies f from which the dipolar couplings can be estimated using the prescription provided earlier. Results of such an experiment carried out with $t_a = 1$ ms and $t_b = 200$ µs are shown in Fig. 4 for the aliphatic carbons of *MBBA*. There are cross peaks occurring at 6.8, 3.8 and 4.0 kHz corresponding to the C_α, C_β, C_γ carbons, which provide the corresponding C–H dipolar couplings as 4.8, 2.7, and 2.8 kHz.

Improved Schemes

Inclusion of homonuclear decoupling during CP

The dipolar oscillations during CP are highly damped due to the couplings among the protons. Consequently the peaks in the two-dimensional spectra are broad and in several instances hard to observe. *Wu et al.* [17] have shown that the use of *Lee–Goldburg* (*LG*) decoupling [18] during cross-polarisation results in the removal of homonulcear dipolar couplings leading to a reduction of the line width along the dipolar axis. The use of the method has been made for the case of the liquid crystal *N*-(4-ethoxybenzylidene)-4-*n*-butylaniline (*EBBA*) [15]. The pulse sequence used for the 2D experiment is shown in Fig. 1c. The t_1 period corresponds to transfer of polarisation from carbons to protons. During this period the proton offset is changed to satisfy the *Lee–Goldburg* condition and carbon power level is adjusted to satisfy the *Hartmann–Hahn* condition so that magnetization exchange takes place under homonuclear proton spin decoupling. The effect of *LG* decoupling resulting in the lengthening of the dipolar oscillation is shown for the case of the benzylidene carbon of *EBBA* in Fig. 5 where results of two experiments, *viz.*, one in which the proton r.f. is applied on-resonance corresponding to normal depolarisation experiment and the other in which *LG* decoupling is employed, are compared.

The homonuclear decoupling during the t_1 period results in the scaling of the heteronuclear couplings, the theoretical scaling factor being $\sin(\theta_m) = 0.82$, where θ_m is the magic angle. The two-dimensional spectrum of *EBBA* was obtained at

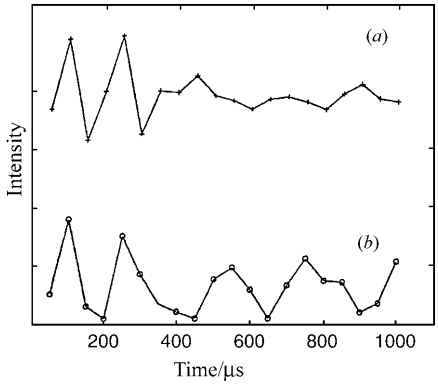

Fig. 5. Intensities of the benzylidene carbon of *EBBA*, as a function of t_1 obtained after *Fourier* transformation along t_2 of the two-dimensional data-set obtained using the pulse scheme shown in Fig. 1c; (a) with on-resonance proton r.f. during t_1 and (b) with *LG* decoupling during t_1

several temperatures using the method and C–H dipolar couplings at several sites were obtained. From the dipolar couplings of the benzylidene carbon, the order parameter of the aromatic core was obtained at these temperatures. Oscillation frequencies were obtained for the aromatic carbons also. From the values of order parameter of the core at different temperatures, the proton–carbon dipolar couplings of the aromatic core can be calculated, assuming a hexagonal geometry of the phenyl ring and fast flip motion about the para axis. In this case, the one bond C–H dipolar coupling D^1_{CH} is nearly the same as the coupling of this carbon to its ortho-proton D^2_{CH} due to the effect of ordering being different along different directions. In such cases, where the carbon is coupled to more than one proton, the evolution of magnetization is expected to proceed in a locked mode [13] and the oscillation frequency is given by $\sqrt{[(D^1_{\mathrm{CH}})^2 + (D^2_{\mathrm{CH}})^2]}$. The values thus calculated and the experimental oscillation frequencies are observed to show a good correlation [15].

Polarisation inversion

As pointed out earlier, Eq. (3) governs the frequencies and intensities of the peaks along the dipolar axis in the 2D experiments. The oscillatory cosine term gives rise to the cross peaks containing dipolar coupling information. There is also the non-oscillatory part which gives rise to the zero frequency peaks, which may overlap with cross peaks close to the center, causing difficulties in measuring small dipolar couplings. For attenuating the zero frequency peaks, use of polarisation inversion instead of cross polarisation has been utilized [16, 17]. The polarisation transfer process for a two spin I-S system can be modeled as a coherent process in mutually commuting zero-quantum and double-quantum manifolds [19]. Under the assumption of high r.f. fields, the dipolar coupling causes as oscillatory evolution of the density matrix in the zero quantum frame, while in the double quantum frame the density matrix remains constant. The former gives rise to the cross peaks and the latter to the axial peak. In polarisation inversion (Fig. 1d) there is an initial polarisation transfer from I spins to S spins during t_a. At the end of this period the two spin system can be taken to be completely polarised due to contact with the proton bath. Thus the initial density matrix $I_Z = I^{\Sigma}_Z + I^{\Delta}_Z$ tends to become $I_Z + S_Z = 2I^{\Sigma}_Z$ where $I^{\Sigma}_Z = 1/2(I_Z + S_Z)$ and $I^{\Delta}_Z = 1/2(I_Z - S_Z)$ are the density operators in the double and zero quantum frames respectively. Inversion of the r.f. field for the S spin corresponds at this point to a change of sign of the S spin Hamiltonian or equivalently the density matrix can be thought of as equal to $I_Z - S_Z = 2I^{\Delta}_Z$. As a result the initial evolution of magnetization during polarisation inversion takes place only in the zero-quantum sub-space. Therefore the dipolar cross-peaks are much more intense than the axial peaks enabling even small dipolar couplings to be observed. At larger contact times, the double-quantum evolution does come into play [16] and the equation governing this process is given by

$$M_S = M_{S0}[1 - \exp(-t_1/T_{II}) - \exp(-3t_1/T_{II})\cos(ft_1)]. \tag{6}$$

Figure 6 shows the contribution to the S spin intensity from the zero quantum and the double quantum evolution as well as the combined effect for both

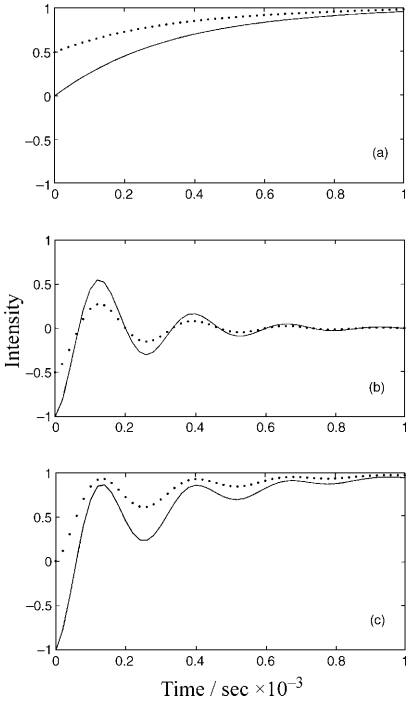

Fig. 6. *S* spin magnetization evolution due to (a) double quantum (b) zero quantum processes, and (c) combined effect of results shown in (a) and (b) during polarisation ($\cdots$) and polarisation inversion (—). The plots correspond to values of f and T_{II} being 3.73 kHz and 333 μs

cross-polarisation and polarisation inversion experiments. It is observed that polarisation inversion leads to a doubling of the amplitude of the oscillatory part and also to a reduction in the initial value of the non-oscillatory component. In a 2D experiment, this would lead to a doubling of the cross-peak intensity and a significant reduction of the axial peak intensity.

A simulation of the relative intensities of the cross-peaks in comparison to the axial peaks for three experiments, namely (i) cross-polarisation, (ii) cross-depolarisation and (iii) polarisation inversion are shown in Fig. 7, using respectively Eqs. (3), (5), and (6). A dipolar coupling of 9.73 kHz and two different values of T_{II} equal to 330 μs and 1 ms were considered. It was observed that polarisation inversion provides the highest relative cross peak intensity for longer values of T_{II} considered, while cross-depolarisation provides higher cross-peak intensity in comparison to cross-polarisation for shorter T_{II} values.

Experimental demonstration of the usefulness of polarisation inversion has been carried out for the case of *MBBA* [16]. 2D spectra obtained using cross polarisation and polarisation inversion are displayed in Fig. 8. In the spectrum obtained using polarisation inversion shown in Fig. 8a, most of the carbon–proton dipolar couplings are observed to be resolved. For several carbons the cross-peaks are much more intense than the axial peaks such that they are not seen in the plot shown in Fig. 8a. Some typical cross-sections are shown in Fig. 9. It is interesting to note that not only short range dipolar couplings of carbons with attached protons

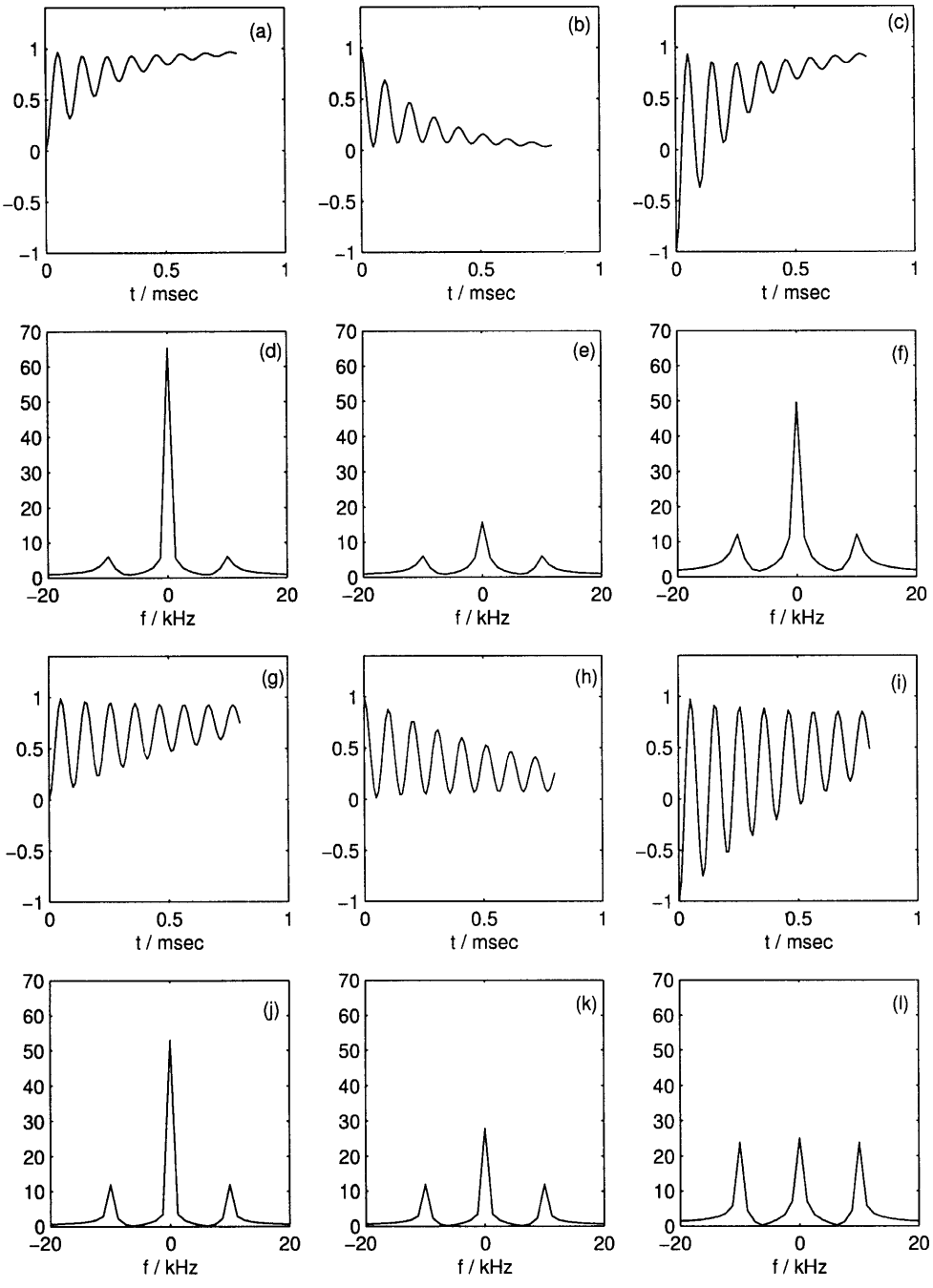

Fig. 7. Comparison of cross-peak intensity versus axial peak intensity for three different cross-polarisation experiments. The time domain signals have been obtained using Eqs. (3), (5), and (6). The corresponding *Fourier* transforms are shown below each. The first, second, and third columns correspond to polarisation, depolarisation, and polarisation inversion experiments. The dipolar coupling used is 9.73 kHz for all the cases. T_{II} is 330 µs for the top two rows and 1 ms for the two bottom rows

could be obtained, but also those of quaternary carbons coupled to remote protons are resolved. This then will lead to useful information on the order parameters of the system studied.

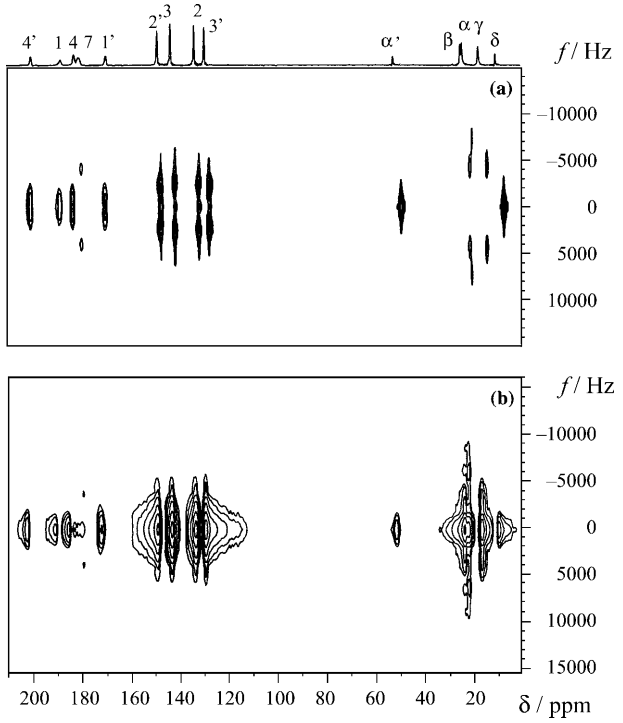

Fig. 8. ^{13}C SLF-2D NMR spectra of *MBBA* in its nematic phase obtained with (a) polarisation inversion and (b) standard cross polarisation pulse schemes on a Bruker DSX-300 NMR spectrometer at room temperature

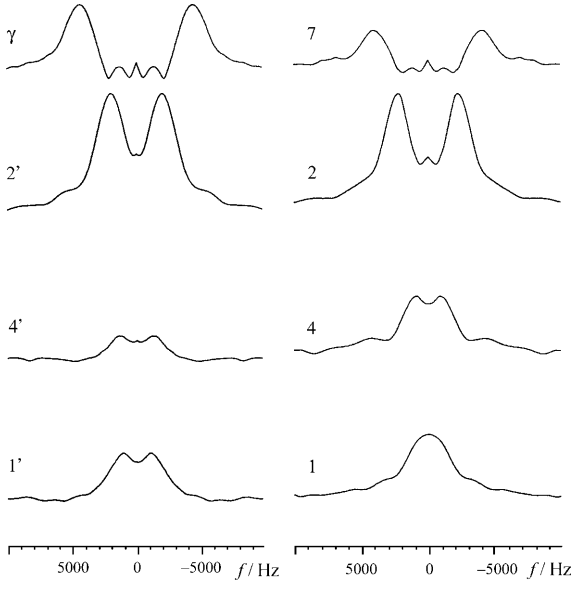

Fig. 9. Plots of cross-sections along the F_1 dimension giving the dipolar oscillation frequencies for γ, 7, 2′, 2, 4′, 4, 1′, and 1 carbons of *MBBA* obtained from the 2D plot shown in Fig. 8a

Cross-Polarisation from the Dipolar Reservoir under Mis-Matched *Hartmann–Hahn* Condition

In the studies reported so far, polarisation transfer has been considered between the *Zeeman* reservoirs of *I* and *S* spins under *Hartmann–Hahn* match. For a mismatch of the *Hartmann–Hahn* condition, an absorptive Lorentzian behavior for the *S* spin intensity has been predicted [19] with the width of the Lorentzian being related to the homonuclear dipolar coupling of the abundant spins. A similar study in which the initial magnetization is in the dipolar bath rather than in the *I* spin *Zeeman* bath has also been reported [20] and on the basis of the quasi-equilibrium theory a dispersive Lorentzian behaviour for the *S* spin intensity has been predicted. The above polarisation transfer process has been considered in detail by carrying out experimental measurements for a range of mismatch conditions by utilizing the pulse scheme shown in Fig. 1e [21]. Here, an ADRF pulse sequence on the *I* spins creates a dipolar order from the *I* spin *Zeeman* order during the period t_a. During t_{CP} a *Hartmann–Hahn* cross-polarisation pulse sequence is used, which results in the transfer of polarisation from the dipolar bath to the *S* spin *Zeeman* bath. The transfer process has the characteristics that *S* spin intensity is zero for $\omega_{1S} = \omega_{1I}$, positive for $\omega_{1S} > \omega_{1I}$ and negative for $\omega_{1S} < \omega_{1I}$ where ω_{1S} and ω_{1I} are the strengths of the spin-lock r.f. on the *S* and *I* spins respectively during the CP process. The *S* spin intensity plotted as a function of $\Delta\omega = \omega_{1S} - \omega_{1I}$ can be shown to be given by

$$M_S = \frac{\beta\lambda^2\Delta\omega}{\Delta\omega^2 + \lambda^2}, \tag{7}$$

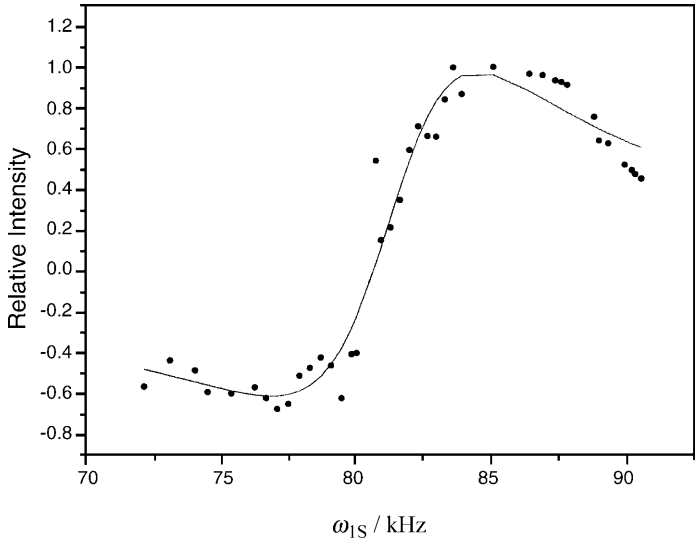

Fig. 10. Variation of cross-polarised signal intensity from the dipolar bath of protons to the α-carbons in the liquid crystal *EBBA* for different r.f. powers (ω_{1S}) on ^{13}C. The experimental points have been obtained by using the pulse sequence of Fig. 1e, with $t_a = t_b = 1$ ms and $t_{CP} = 200\,\mu$sec. The spectra were obtained on a Bruker DSX-300 NMR spectrometer at a ^{13}C resonance frequency of 75.43 MHz. The proton r.f. power (ω_{1I}) was kept constant at 83 kHz. The continuous curve corresponds to a fit of the experimental data to a mixture of dispersive and absorptive Lorentzian functions and yields a value of $\lambda^2 = 14.2\,\text{kHz}^2$ for the α carbon

where β is the initial inverse spin temperature of the dipolar reservoir and λ^2 is related to the *I* spin second moment. The experimental results for the α carbon of *EBBA* in its oriented phase obtained by observing the ^{13}C resonance and by using the pulse sequence of Fig. 1e are shown in Fig. 10. The points correspond to the intensity of the carbon line as a function of ω_{1S} for a fixed value of ω_{1I}.

It is observed that the plot indeed shows an overall dispersive Lorentzian behaviour. However, the fit of the data to Eq. (7) showed some deviations. A better fit to the experimental data could be obtained by including an additional adsorptive Lorentzian of the same width which could arise due to transfer from remnant *Zeeman* magnetization of the *I* spins at the end of the ADRF period, cross polarising directly to the *S* spins [21]. This continuous curve shown in Fig. 10 corresponds to the fit obtained using the above procedure. A value 14.2 kHz^2 for λ^2 has been obtained for the α carbon of *EBBA*. Other methylene carbons along the chain show a variation of λ^2 that is expected on the basis of the variation of the local order parameters of the system. This method like the WISE technique [22], provides a means of indirectly monitoring proton dipolar couplings using the heteronuclear chemical shift dispersion.

Applications

The cross-polarisation techniques mentioned above have been utilized to obtain dipolar couplings and order parameters in several novel liquid crystalline systems such as:

(i) Aromatic systems containing four rings in the main core, a lateral hexyloxy chain, and a lateral aromatic branch with the aromatic ring itself being modified by different substitutents at *meta* or *para* position [23].
(ii) Systems containing four rings in the main core, one terminal, and two nearby lateral chains on each of the outer aromatic rings [24].
(iii) Molecules containing the 2-phenylindazole core – the first bonds of the two terminal chains on the either side are not along the same axis due to the presence of the five membered ring in the core [25].

As an illustration of the use of the C–H bond order parameter obtained from utilizing the cross polarisation technique, systems containing three aromatic rings with a lateral crown-ether fragment and with oxyethylene (*OE*) units replacing the terminal alkoxy chains is presented [26] here. The replacement of the alkoxy chains by chains containing the oxyethylene units decreases the melting and clearing temperature so as to obtain nematic compounds near room temperature. The symmetric mesogen containing one *OE* unit in the terminal chain, referred to as *CINPOE*1*Bu* (Fig. 11) has been studied. The ^{13}C chemical shifts in the isotropic phase and in the nematic phase at different temperatures have been monitored. The SLF 2D spectrum of the compound in its nematic phase at 349 K obtained using the pulse sequence of Fig. 1d is shown in Fig. 11. From the peaks in dipolar dimension, the magnitude of the dipolar interaction for several carbons have been obtained.

For example, carbon C_a and C_c have the same chemical shifts, but have different dipolar couplings, the larger one being attributed to C_a, the first carbon in the terminal chain. In the crown-ether segment, it is noticed that the dipolar couplings decreases from C_α to C_γ, but increases for C_δ. This indicates that the average angle

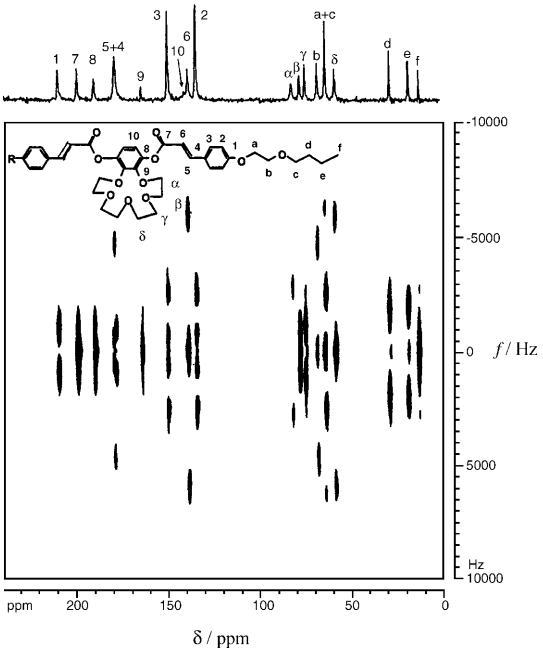

Fig. 11. ^{13}C 2D spectrum of *CINPOE1Bu*, a liquid crystal containing a crown-ether and an oxyethylene unit in its nematic phase at 349 K, recorded on a Bruker DSX-300 NMR spectrometer at 75.47 MHz

between the C–H bond and the long molecular axis is less than the magic angle for carbons, C_α, nearer to the magic angle for C_β and C_γ and greater than magic angle for C_δ. This conclusion is supported by molecular modelling studies of the central part of a single molecule. For carbons in the polyoxyethylene chain, it is expected that the order parameter decreases monotonically with increasing distance from the core. This is in contrast to the odd–even effect usually observed in a terminal alkyl or alkoxy chain. Such a difference arises due to different probabilities for the conformers of the *POE* chain [27, 28]. In the system under consideration with one *OE* unit and one butyl fragment, the dipolar couplings decreases monotonically over the *OE* segment from carbon *a* to *c* while for the remainder of the carbons (*d* to *f*) the odd–even effect is present. The variation of the bond order parameter with temperature shows interesting correlation with the corresponding chemical shift of the carbon. A linear correlation between chemical shift and order parameter indicates that the conformation does not change significantly in the temperature range studied. Such a linear correlation has been observed for the carbons of the lateral crown-ether. On the other hand, the non-linear correlation observed for the carbons of the *OE* unit indicates that the conformational probabilities change significantly with temperature resulting in different averaged values of the dipolar couplings and chemical shift anisotropies.

Conclusions

The coherent effects of the cross-polarisation have been shown to provide detailed information on dipolar couplings in nematic liquid crystalline systems. The information thus obtained enables estimation of the order parameters of the liquid

crystals. Several variants of the standard cross polarisation experiments were presented and their utility discussed. Typical applications of the method were presented. In addition to the above studies where heteronuclear dipolar couplings were used, another cross-polarisation method that can provide information about the proton–proton dipolar couplings was examined, thus providing another means of obtaining local order.

Acknowledgement

The authors would like to thank Prof. Anil Kumar for useful suggestions.

References

[1] Diehl P, Khetrapal CL (1969) NMR: Basic Principles and Progress **1**: 1
[2] Emsley JW (1985) Nucl Magn Reson Liq Cryst. Reidel, Dordrecht
[3] Dong RY (1994) Nucl Magn Reson Liq Cryst. Springer, New York
[4] Hohener A, Muller A, Ernst RR (1979) Mol Phys **38**: 909
[5] Magnuson ML, Tanner LF, Fung BM (1994) Liq Cryst **16**: 857
[6] Magnuson ML, Fung BM, Schadt M (1995) Liq Cryst **19**: 333
[7] Courtieu J, Bayle JP, Fung BM (1994) Prog Nucl Magn Reson Spectrosc **26**: 141
[8] Fung BM (1996) Encyclopedia of NMR **4**: 2744
[9] Caldarelli S, Hong M, Emsley L, Pines A (1996) J Phys Chem **100**: 18696
[10] Hong M, Pines A, Caldarelli S (1996) J Phys Chem **100**: 14815
[11] Caldarelli S, Lesage A, Emsley L (1996) J Am Chem Soc **118**: 12224
[12] Muller L, Anil Kumar, Baumann T, Ernst RR (1974) Phys Rev Lett **32**: 1402
[13] Hester RK, Ackerman JL, Cross VR, Waugh JS (1975) Phys Rev Lett **34**: 993
[14] Pratima R, Ramanathan KV (1996) J Magn Reson **A118**: 7
[15] Nagaraja CS, Ramanathan KV (1999) Liq Cryst **26**: 17
[16] Neeraj Sinha, Ramanathan KV (2000) Chem Phys Lett **332**: 125
[17] Wu C, Ramamoorthy A, Opella SJ (1994) J Magn Reson **A109**: 270
[18] Lee M, Goldburg WI (1965) Phys Rev **A140**: 1261
[19] Levitt MH, Suter D, Ernst RR (1986) J Chem Phys **84**: 4243
[20] Zhang S, Stejskal EO, Fornes RE, Wu X (1993) J Magn Reson **A104**: 177
[21] Venkatraman TN, Neeraj Sinha, Ramanathan KV (2002) J Magn Reson **157**: 137
[22] Schmidt-Rohr K, Clauss J, Spiess HW (1992) Macromolecules **25**: 3273
[23] Berdague P, Bayle JP, Fujimori H, Miyajima S (1998) New J Chem 1005
[24] Berdague P, Munier M, Judeinstein P, Bayle JP, Nagaraja CS, Ramanathan KV (1999) Liq Cryst **26**: 211
[25] Berdague P, Judeinstein P, Bayle JP, Nagaraja CS, Neeraj Sinha, Ramanathan KV (2001) Liq Cryst **28**: 197
[26] Neeraj Sinha, Ramanathan KV, Berdague P, Judeinstein P, Bayle JP (2002) Liq Cryst **29**: 449
[27] Rayssac V, Judeinstein P, Bayle JP, Kuwahara D, Ogata H, Miyajima S (1998) Liq Cryst **25**: 427
[28] Samulski ET, Dong RY (1982) J Chem Phys **77**: 5090